Su, Andrew R., The Effect of Tooth Loss on Craniofacial Morphology. Master of Science (Medical Sciences – Anatomy), May 2021

Tooth loss (edentulism) is known to reduce biomechanical loading of the face, resulting in changes in craniofacial morphology and bone material properties. However, the effect of tooth loss on masticatory muscles and their bony attachments is less clear. We hypothesize that the craniofacial shape changes in humans following tooth loss are related to alveolar resorption in both the mandible and maxilla. We also anticipate a recession of bone at the insertion sites of the masticatory muscles, namely the zygomatic arch and mandibular ramus.

CT scans (≥70 years) were obtained from the New Mexico Decedent Imaging Database. Edentulous individuals (0 teeth, n=10/sex) were compared to functionally dentate individuals (≥20 teeth, n=10/sex). 3D Slicer software was used to collect 3D fixed and sliding landmarks along the mandible and facial skeleton. A general Procrustes analyses (GPA) and principal components analyses (PCA) were used to compare the morphology of the two populations.

Results show significant differences in facial and mandibular shape between the two groups. Between the sexes, shape differences followed similar tends between dentate and edentate individuals. However, the magnitude of these differences varied between the sexes. Variation within edentulous individuals suggests that the time since tooth loss and behavioral factors (e.g. denture wearing) may impact the degree of alveolar resorption. A superior elongation and posterior retraction of the coronoid process was observed in edentulous individuals, suggesting greater relative atrophy of the temporalis muscle relative to the masseter following tooth loss. Future studies will investigate the impact of tooth loss on chewing muscle morphology and force production.

THE EFFECT OF TOOTH LOSS ON CRANIOFACIAL MORPHOLOGY

Andrew R. Su, B.S.

Approved:

Rachel Menegaz, Ph.D., Major Professor

Scott Maddux, Ph.D., Committee Member

Emma Handler, Ph.D., Committee Member

Johnathan Tune, Ph.D., Chair, Department of Physiology & Anatomy

Caroline Rickards, Ph.D., Program Director, Medical Sciences Research Track

Lisa Hodge, Ph.D., Chair, Assistant Dean, Specialized MS Programs

J. Michael Mathis, Ph.D., Ed.D., Dean, Graduate School of Biomedical Sciences

THE EFFECT OF TOOTH LOSS ON CRANIOFACIAL MORPHOLOGY

INTERNSHIP PRACTICUM REPORT

Presented to the Graduate Council of the

Graduate School of Biomedical Sciences

University of North Texas

Health Science Center at Fort Worth

in Partial Fulfillment of the Requirements

For the Degree of

MASTER OF SCIENCE

By

Andrew R. Su, B.S.

Fort Worth, Texas

May 2021

ACKNOWLEDGEMENTS

First, I would like to thank my principal investigator and major professor, Dr. Rachel Menegaz, for her wonderful mentorship throughout this practicum. Her patience, understanding, and enthusiasm have driven my growth both in the research lab and in the classroom. Her good humor and seemingly miraculous ability to always have a meme ready for every situation were bright spots in a challenging year.

I would next like to thank my advisory committee, Dr. Scott Maddux and Dr. Emma Handler, for their support and guidance. Their direction and feedback have been deeply appreciated. I also would like to thank my fellow lab members, Graci Finco, Courtney Miller, and Dr. Rex Mitchell for creating a welcoming space for me as I made my first forays into anatomical research. I would particularly like to thank Rex for all of his help with developing this project.

Thank you to the New Mexico Decedent Image Database for providing CT images for this study.

To my friends who have always there for me, I offer my deepest gratitude. I would lastly like to thank my family, who have always offered unwavering support in the course of my educational pursuits.

TABLE OF CONTENTS

LIST OF TABLES

LIST OF FIGURES

CHAPTER 1: INTRODUCTION

Craniofacial morphology is subject to a variety of influences, not least of which are conditions that induce a loss of function. Muscles, and specifically the muscles of mastication, may undergo many structural and physiological changes in response to normal aging as well as to pathological conditions such as tooth loss or myasthenia gravis. Altered loading patterns caused by these muscular changes may induce changes in the bony structures of the face. While changes to craniofacial morphology have been characterized well in animal models, in humans these observations have been limited to changes in facial bone dimensions and masticatory muscle size.

This practicum focuses on investigating the effects of tooth loss on the craniofacial morphology of adult human anatomical donors above age 70. Edentulism, or tooth loss, can be viewed as a proxy for unloading of the masticatory muscles. While the effects of unloading on bone and muscle fiber phenotype are well characterized in human limb and trunk muscles, its effects on masticatory muscle phenotype are less clear.

Table 1: List of Abbreviations

Abbreviation	**Explanation**
GPA	General Procrustes Analysis
H&E	Hematoxylin & Eosin
IHC	Immunohistochemistry
MyHC, MHC	Myosin Heavy Chain
NMDID	New Mexico Decedent Image Database
PCA	Principal Components Analysis
SDS-PAGE	Sodium Dodecyl Sulfate-Polyacrylamide Gel Electrophoresis

CHAPTER II: INTERNSHIP SUBJECT

BACKGROUND

Section 1: Tooth Loss and the Craniofacial Skeleton

The bony structures of the face and jaw are subject to changes in size and shape in response to various stimuli. Edentulism, or tooth loss, has been found to have wide-ranging effects on the skull.[1] Tooth loss as a result of disease and lifestyle factors results in the resorption of alveolar bone, where teeth insert into a peg and socket joint known as a gomphosis.[2,3] The process of bone loss also increases with age as the rate of bone production by osteoblasts decreases relative to the rate of bone resorption by osteoclasts.[4] Aging compounds the disuse effect seen in edentate individuals, thus leading to dramatic alveolar recession.[4] Total facial height is known to be reduced in individuals with tooth loss.[5,6] A more recent study showed that upper facial height, defined as the height of the face superior to the basal portion of the maxillary bone,[5] is also reduced in individuals with tooth loss.[1] However, it is unclear if the decreased facial height found by these studies is directly related to alveolar resorption or the product of more widespread changes to the facial skeleton. Furthermore, edentulous individuals have a more hyperbolic-shaped palate as compared to dentate individuals.[1] Interestingly, edentulism has no pronounced effects on the gross morphology of the zygomatic arch, despite it being the origin of the masseter muscle, a key jaw-closing muscle.[1]

In addition to gross morphological changes, edentulism has also been found to alter the cross-sectional and material properties of cortical bone in the facial skeleton. Edentulous individuals have relatively thinner cortical bone throughout the upper facial skeleton as compared to dentate individuals.[7] The maxilla undergoes the greatest changes, with decreases in stiffness, resistance to elastic deformation, and density.[7] Altered material properties were also

found in the frontal bone around the orbit, the zygomatic bone around the orbit, and in the zygomatic arch, suggesting that despite a lack of gross morphological change, histological changes are still occuring.[7]

Edentulism is also noted to have profound effects on the mandible. Alveolar resorption in edentulous individuals is well characterized, with the rate of resorption being greater at the buccal surface as compared to the lingual surface.[8] The degree of buccal resorption was noted to be greater at the molars than at the premolars or incisors.[8] Changes in material properties as a result of edentulism were also observed in the mandible. The mandibular cortical bone of edentulous individuals was noted to have thinner inferior mandibular margins and thicker mandibular symphyses as compared dentate individuals.[9] These seemingly contradictory shifts in cortical bone thickness suggest that edentulism fundamentally alters the functional bone stresses experienced by the mandible.[9]

Section 2: Identification of Human Muscle Fibers

Human skeletal muscle is a heterogeneous mixture of various muscle fiber types.[10] These muscle fiber types can be characterized in several ways: morphologically, physiologically, histologically, biochemically, and neurologically (Table 2).[11]

Initially, whole muscles were generally categorized as fast or slow based upon contraction velocity, with fast muscles appearing white in color and slow muscles appearing red.[12] This difference in color is attributed to the relative proportion of myoglobin and degree of capillarization within the muscle, and thus indicative of the muscle's oxidative capacity.[12] It is important to note that as contraction velocity increases, that muscle's oxidative capacity and endurance decreases.[11] Thus faster fibers have lower endurance and oxidative capacity, while slower fibers have higher endurance and oxidative capacity.[11]

Histochemical staining for myosin ATPase takes advantage of the differing pH sensitivities of each myosin ATPase.[10] This technique has led to the identification of 7 human muscle fiber types, with types I, IIA, and IIB being the originally identified fiber types, and types IC, IIC, IIAC, and IIAB later identified as having intermediate staining characteristics.[10] These types, ordered from slowest to fastest, are as follows: I, IC, IIC, IIAC, IIA, IIAB, and IIB.[13] Muscle fiber size proves an unreliable way of classifying fiber type, as type IIA fibers are typically the largest in males, while in females, type I fibers are either larger or of similar size as type IIA fibers.[14]

Myosin heavy chain isoforms are identified via immunohistochemical analysis with anti-myosin antibodies or via SDS-PAGE.[13] There only three myosin heavy chain isoforms expressed in human limb muscles are MyHCI, MyHCIIa, and MyHCx/d, and they correspond to myosin ATPase types I, IIA, and IIB respectively.[10] The intermediate myosin ATPase fiber types can be explained by the fact that each muscle fiber has the potential to contain more than one myosin heavy chain isoform.[11] Thus, while the pure fibers express only express one myosin heavy chain isoform, intermediate or mixed fibers co-express neighboring myosin heavy chain isoforms in varying proportions.[10,15]

Biochemical identification combines myosin ATPase histochemistry with metabolic enzyme histochemistry in order to classify muscle fibers.[15] These metabolic enzymes are associated with either aerobic/oxidative pathways or anaerobic/glycolytic pathways.[13] When combined with myosin ATPase histochemistry, this yields three fiber types: slow oxidative, fast-twitch oxidative, and fast-twitch glycolytic.[15]

One final way of identifying muscle fibers is via their associated motor unit.[16] A motor unit is defined as an α-motoneuron and all muscle fibers that it innervates.[16] As a result, motor

units can also be divided into groups based upon their contractile velocity and rate of fatigue: slow-twitch, fast-twitch fatigue resistant, fast-twitch fatigue-intermediate, and fast-twitch fatigable.[11,16]

Table 2: Summary of Trends for Identification of Human Muscle Fibers

Contraction Velocity	Slow		Fast				
Color	Red		White				
Myosin ATPase IHC	Type I	Type IC	Type IIC	Type IIAC	Type IIA	Type IIAB	Type IIB
MyHC Isoform ID	MyHCI	MyHCI + MyHCIIa			MyHCIIa	MyHCIIA + MyHCIIx/d	MyHCIIx/d
Biochemical	Slow-Twitch Oxidative				Fast-Twitch Oxidative		Fast-Twitch Glycolytic
Motor Unit	Slow-Twitch				Fast-Twitch Fatigue-Resistant	Fast-Twitch Fatigue-Intermed.	Fast-Twitch Fatigable

Section 3: Plasticity of Human Skeletal Muscle

Human bone and skeletal muscle exhibit great plasticity and are able to adapt their contractile and metabolic properties in response to changes in demand.[15] An important component of this plasticity is fiber type conversion, with the conversion between type IIB and IIA being the most common.[15]

Deconditioning, which includes physiological changes in muscle fibers resulting in decreased muscle size, strength, and endurance, as a result of disuse, is typically associated with the conversion of slow-type fibers to fast-type fibers.[11] Similar observations have been noted in human subjects following microgravity exposure, spinal cord injury, and detraining.[15] In addition to a slow-to-fast fiber type transitions, decreased use of skeletal muscle is associated with a decrease in the levels of enzymes associated with aerobic-oxidative metabolism.[15]

In contrast, endurance training can change the composition of myosin heavy chains within a muscle fiber.[17] A study done with endurance-trained athletes focused on evaluating this difference within the vastus lateralis.[17] Within type II fibers, the proportion of slower-type MyHCIIa increases relative to that of faster-type MyHCx/d, thus causing an increase in the proportion of type IIA fibers.[17] While type II fibers do not seem to convert to pure type I fibers, there is an increase in the proportion of type I and type IIA hybrid fibers.[17] In high-intensity resistance training, similar changes are observed, but muscle hypertrophy is the primary contributor to increased contractile strength.[18] However, endurance training is associated with increased oxidative capacity in all fiber types due to increased amounts of mitochondria, aerobic-oxidative metabolic enzymes, and capillarization, while high-intensity resistance training is not.[19]

Age-related changes in muscle differ from deconditioning in that loss of muscle performance is primarily due to selective atrophy of certain muscle fiber types rather than conversion of muscle fibers.[20] While there is a decrease in the total numbers of both type I and type II fibers, type II fibers preferentially atrophy, causing a relative increase in the number of type I fibers.[21,22] Additionally, age-associated α-motoneuron loss may lead to some muscle fibers becoming reinnervated by neighboring motor units of a different type, causing a conversion of that muscle fiber to the type of the new motor unit.[23] This may explain why older individuals have a greater proportion of muscle fibers that co-express MyHCI and MyHCIIa relative to the muscles of younger individuals.[24] Aging is also associated with changes in type II muscle fibers, which can be 10%-40% smaller in size than in younger individuals.[25] However, these changes were not seen in type I muscle fibers.[25]

Section 4: Differences between Human Masticatory Muscles and Muscles of the Limb and Trunk

The masticatory muscles differ from limb and trunk muscles in many ways. While limb and trunk motor systems are responsible for relatively simple motor tasks, the jaw muscles are responsible for a much larger variety of motor tasks.[26] This is thought to explain why jaw muscles contain an abundance of hybrid fibers, which are typically only found in limb and trunk muscles during disuse, extreme use, transition, or regeneration.[27] Additionally, some masticatory muscle fibers co-express MyHC-fetal or MyHC-cardiac α, isoforms that are not typically expressed in limb or trunk muscles.[26] The size of jaw muscle fibers is also unusual, with type II fibers tending to have a smaller cross-sectional area than type I fibers – the reverse is true of limb and trunk muscles.[28]

Even within jaw muscles, there is there is some variability with fiber-type composition. Fibers in jaw-closing muscles express a much greater proportion MyHCI than jaw-opening

muscles.[29] Jaw-closers also contain significantly more hybrid fibers overall than jaw-opening muscles.[28] Jaw-opening muscles tend to have fibers containing a greater proportion of MyHCII than jaw-closers.[28] These differences suggest that jaw-closing muscles are better adapted to performing slow, repetitive motions and smooth, graded force production, while the jaw-opening muscles are better adapted to performing fast, phasic movement.[28] Jaw-closers are also responsible for maintaining the resting position of the mandible against gravity, indicating that the fiber type composition of jaw-closers is indicative of its higher level of daily activity.[30]

Section 5: Plasticity of Masticatory Muscle

The effects of dietary changes on masticatory muscle fiber phenotype have been studied extensively in animal models. Rats that consumed a soft diet composed of feed pellets dissolved water tended to have relatively more Type IIB fibers and relatively fewer Type IIA and transitional fibers as compared to animals that consumed a hard diet composed of normal feed pellets, suggesting that unloading the masticatory apparatus induces a general shift from slower fibers to faster fibers.[31] Additionally, Type II fibers in the masseter of rats fed a soft diet were noted to be smaller in diameter than those of rats fed a hard diet.[31]

In rhesus monkeys, edentulous specimens were noted to have significantly fewer slow-twitch fibers and more fast-twitch fatigable fibers in the posterior masseter, anterior temporalis, and posterior temporalis muscles as compared to specimens with functional dentition, suggesting a general transition from slower fibers to faster fibers.[32] Slow-twitch fibers in edentulous specimens were also noted to be significantly smaller than slow-twitch fibers in specimens with functional dentition, but no discernible difference in size was observed in fast-twitch fatigue resistant or fast-twitch fatigable fibers.[32]

In rabbits, animals fed a hard diet had significantly larger slow-MyHC fibers relative to those fed a soft diet.[33] This is confirmed in another study, which demonstrated that animals with increased load on the masticatory apparatus develop larger masseters.[34] However, the findings of this study differ from those of the rat and monkey studies – rabbit masseters in specimens with increased load have an absolutely and relatively lower number of slow, type I fibers and relative increases in the number of fast, type II fibers, suggesting increased load is associated with a slow to fast transition.[34] Interestingly, another study done in rats found similar results – animals with increased loading tended to have smaller type I fibers and more type II fibers.[35]

While human studies have been limited in scope, there is evidence that edentulism is associated with smaller masseters, both in length and width.[36] In the course of our literature review, no studies were found addressing what fiber type changes might occur as a result of edentulism in humans. This present study aims to address this gap in the literature.

SPECIFIC AIMS

The specific aims of this study are:

(1) to determine if significant differences in craniofacial dimensions are present in edentulous samples as compared to dentate samples

H1A: We hypothesize that edentulous individuals will have decreased alveolar height in the maxilla and mandible relative to individuals with functional dentition due to bone resorption.

H1B: We hypothesize that edentulous individuals will have decreased facial height relative to functional edentulous individuals and that this height decrease will be driven by alveolar resorption.

H1C: We hypothesize that the muscle attachment sites at the zygomatic arch and mandibular ramus of edentulous individuals will be reduced relative to attachment sites in a functionally dentate individual due to decreased function of the masticatory muscles.

(2) to determine if significant differences in masseter fiber phenotype are present in edentulous samples as compared to dentate samples

H2A: We hypothesize that there will be a reduction in the size of muscle fibers in the masseter in edentulous individuals relative to functionally dentate individuals.

H2B: We hypothesize that there will be a relative increase in the proportion of fast-twitch (type II) fibers versus slow-twitch (type I) fibers, as suggested by previous unloading studies in mammal limb and trunk muscles.

SIGNIFICANCE

Our understanding of the effects of unloading of limb and trunk muscles on both the bony skeleton as well as muscle phenotype is well-established in the literature. However, less is known about the effects of unloading on the musculoskeletal tissues of the cranium. Previous studies on edentulism done in humans focused on changes to the alveolar bone and facial skeleton, or on masticatory muscle volume. There is limited information on what changes, if any, are seen in the morphology of muscle attachment sites or in masticatory muscle fiber phenotype following tooth loss in humans. Animal studies have not produced a clear consensus on the effect that edentulism has on masticatory muscle fiber phenotype. The present study seeks to address this gap in the literature.

MATERIALS AND METHODS

Section 1: CT Imaging and Landmark Collection

3D imaging studies of 20 edentate (10 male/10 female) and 20 functionally dentate (10 male/10 female) of age 70 or older were obtained from the New Mexico Decedent Image Database (Table 3). Individuals were considered edentate only if they had zero teeth. Individuals were considered functionally dentate if they had 20 or more of 32 teeth. Individuals with 1-19 teeth were excluded, and we attempted to exclude those with implants. 3D Slicer software was used to generate 3D models (Volume Rendering module) and to collect digital craniofacial landmarks (Markups module). A total of 14 fixed landmarks and 29 sliding landmarks were placed on the cranium. These curves approximated the lower portion of the nasal aperture, the curve of the maxillary alveolar bone, the inferior aspect of the zygomatic arch, the superior aspect of the zygomatic arch, and the lower portion of the orbit (Figure 1, Table 4). A total of 9 fixed landmarks and 43 sliding landmarks were placed on the mandible. These curves approximated the height of the mandible at the mandibular suture, the inferior border of the mandibular corpus and posterior border of the mandibular ramus, the mandibular notch, and the superior border of the mandibular corpus and anterior border of the mandibular ramus (Figure 2, Table 5).

Table 3: Demographics of NMDID Craniofacial CT Scans

	Edentulous	**Dentate**	**Age Range**	**Mean Age**
Female	10	10	70 - 90	80 ± 7.08
Male	10	10	70 - 91	78.25 ± 6.21
Total	20	20		

Figure 1: Cranial Landmarks

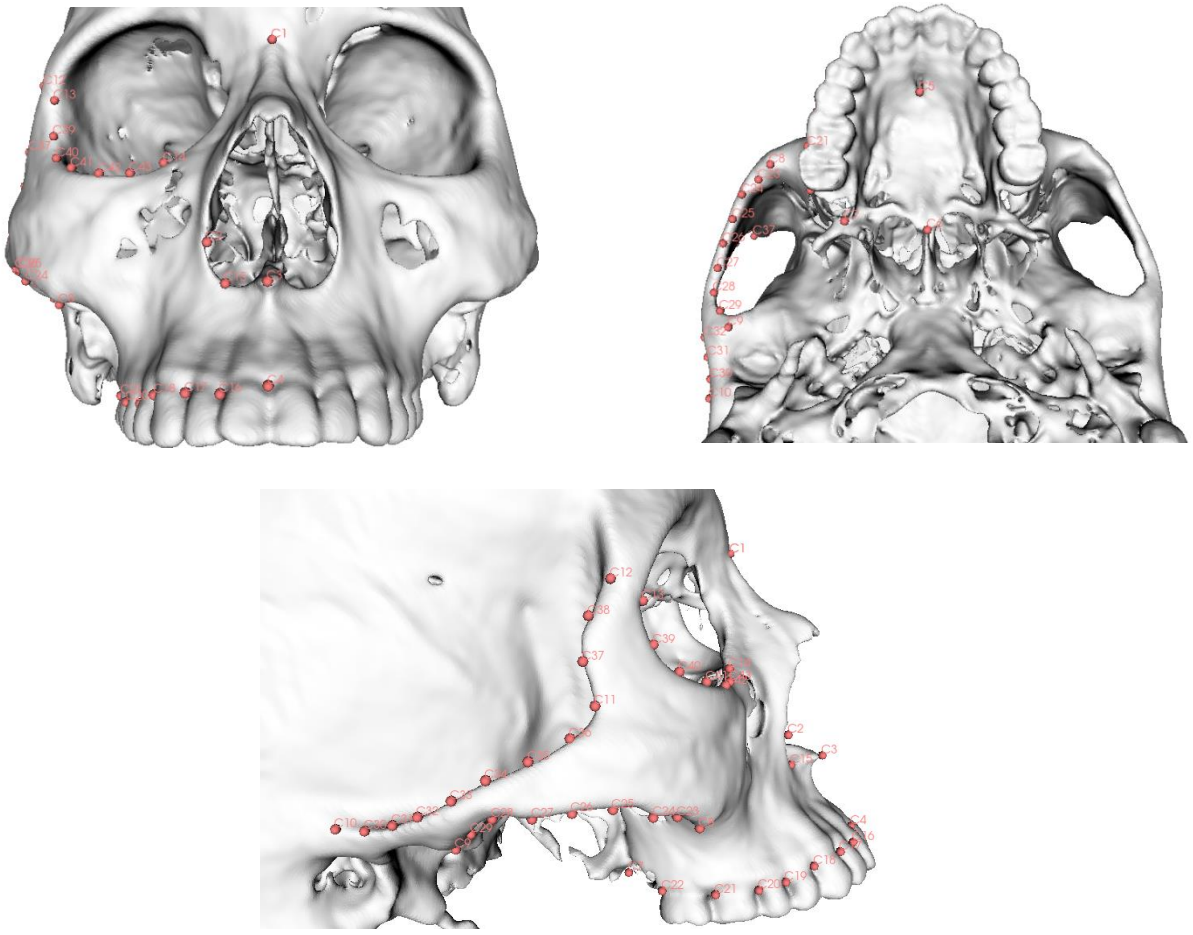

Table 4: List of Cranial Landmarks and Semi-Landmarks

Cranial Landmarks	
Number	**Landmark**
1	Nasion
2	Alare
3	Anterior nasal spine
4	Prosthion
5	Incisive foramen
6	Caudal nasal spine

7	Maxillary tuberosity
8	Inferior anterior root of the zygomatic arch
9	Articular eminence
10	Radiculare
11	Superior zygotemporale
12	Frontomalare temporale
13	Frontozygomatic orbitale
14	Lacrimomaxillary suture
15	Landmark between alare and anterior nasal spine, along the piriform aperture
16-22	Landmarks between prosthion and maxillary tuberosity along the inferior aspect of the maxilla
23-29	Landmarks between the inferoanterior root of the zygomatic arch and the articular eminence, along the inferior aspect of the zygomatic arch
30-36	Landmarks betweeen radiculare and superior zygotemporale, along the superior aspect of the zygomatic arch
37-38	Landmarks between superior zygotemporale and frontomalaretemporale, along the zygomatic bone
39-43	Landmarks between frontozygomatic orbitale and lacrimomaxillary suture, along the inferolateral aspect of the orbit

Figure 2: Mandibular Landmarks

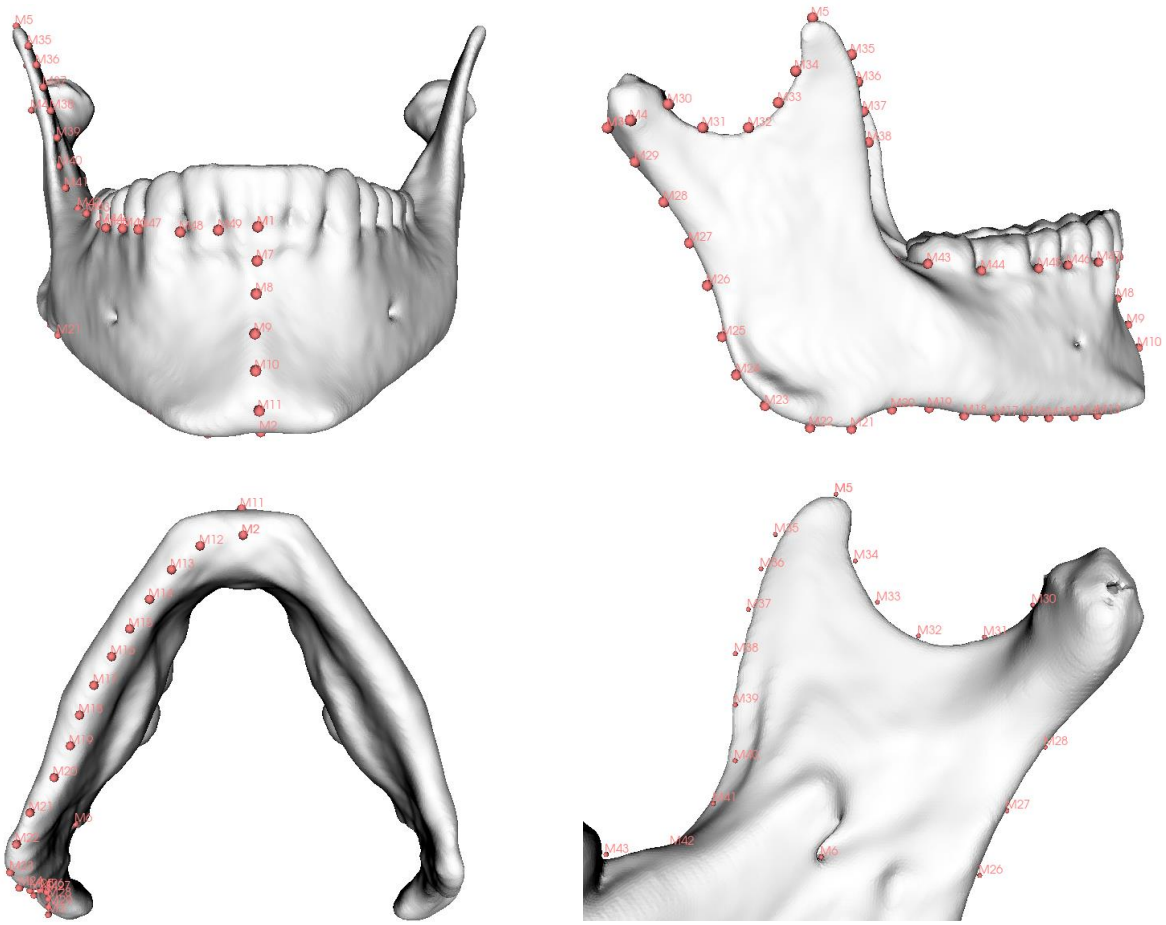

Table 5: List of Mandibular Landmarks and Semi-Landmarks

Mandibular Landmarks	
Number	**Landmark**
1	Infradentale
2	Gnathion
3	Condylion superior
4	Condylion laterale
5	Apex of the coronoid process
6	Anterior border of the mandibular foramen

7-11	Landmarks between infradentale and gnathion, along the mandibular suture
12-29	Landmarks between gnathion and condylion superior, along the inferior border of the mandibular body and posterior border of the ramus
30-34	Landmarks between condylion laterale and the apex of the coronoid process, along the mandibular notch
35-49	Landmarks between the apex of the coronoid process and infradentale, along the anterior medial border of the ramus and superior border of the mandibular body

A repeatability study was performed using 3 edentate and 3 dentate specimens. 3 replicates were performed per specimen. The Geomorph package in RStudio was used to perform GPA and PCA. Procrustes ANOVA was used to assess the contribution of inter-replicate variation to total variation. The r-squared value for the cranium was 0.9366, meaning that 93.66% of the variation was inter-individual and the remaining 6.34% of variation was due to inter-replicate variation. The r-squared value for the mandible was 0.9329, meaning that 93.29% of the variation was inter-individual and the remaining 6.71% of variation was due to inter-replicate variation.

Section 2: Statistical Analysis

The Geomorph package in R Studio was used to perform General Procrustes Analyses and Principal Components Analyses. Shapes between the groups as well as interactions between shape and sex were compared using Procrustes ANOVA.

Principal components were visualized as lollipop graphs, which show the direction of those shape differences – the sphere is the mean shape, and the stick is the direction in which edentulous individuals differ from that mean.

Section 3: Tissue Collection

Samples were collected from embalmed human anatomy donors through the University of North Texas Health Science Center Willed Body Program following a dissection-based anatomy course. Tissue was harvested from the most intact masseter and fixed in 10% neutral buffered formalin for 48 hours, then stored in 70% ethyl alcohol at 4°C. 13 edentulous and 2 dentate masseters were collected from the donors available in the 2019-2020 gross anatomy courses. Tissue collection is ongoing and ultimately, we aim to have n=15 for each group.

Section 4: Fiber Type Analysis

We attempted to quantify changes in muscle fiber type using fluorescent immunohistochemistry (IHC). Sequential paraffin-embedded sections (10 μm) were taken from each masseter sample along an anteroposterior axis. Sections were stained with hematoxylin and eosin (H&E) for qualitative analysis of cell morphology and integrity. To identify muscle fiber types, deparaffinized sections were stained with a primary antibody (ab 91506) for fast isoforms of the myosin heavy chain, and a secondary fluorescent antibody (ab 150077). DAPI nuclear stain was used as a tertiary antibody. Primary controls used rabbit IgG (vector 1-1000) and PBS in place of the primary antibody. Stained and control slides were imaged in the UNTHSC Microscopy Core Facility on a Zeiss confocal microscope at 10x magnification.

We had intended to use ImageJ to quantify the number and cross-sectional areas of stained fibers (containing fast MyHC) and unstained fibers (containing slow MyHC). However, the imaged slides proved to be unsuitable for data collection. Due to unforeseen circumstances

that caused the microscopy core to be shut down in December 2020 (COVID-19) and February 2021 (flooding from Winter Storm Uri), the integrity of our samples was compromised. Delayed imaging resulted in the degradation of the secondary fluorescent antibodies and poor contrast between stained and unstained cells. While we did consider using fiber size as a proxy for fiber type, the trends are different for males and females and the muscle fibers of each sex are influenced differently by aging, making this an unreliable determinant of muscle fiber type.[14,25] We therefore were unable to proceed with our planned IHC analysis of muscle fiber type, and ultimately decided to invest our time and energy in the geometric morphometric analyses of the craniofacial skeleton. Histological analyses of the collected tissue will be conducted at a later date when circumstances are more conducive to this methodology.

Section 5: Limitations

We acknowledge the possibility of intra-observer and inter-observer variability due to manual landmarking of the 3D models of the specimens. The variable quality of the NMDID CT scans contributes to this, as the presence of medical devices and dental fillings producing interference in the imaging studies were an impediment to data collection. Collecting landmark data in edentulous individuals proved particularly challenging due to the loss of convenient visual landmarks and marked shape changes. Variations due to sex, age, socioeconomic, and behavioral factors such as denture wearing are also not accounted for in this study.

Due to muscle atrophy, we may be unable to differentiate between superficial and deep masseter specimens. Additionally, we will be unable to quantitatively identify hybrid muscle fibers due to the limitations of our antibodies. There were significant limitations on muscle data analysis due to the circumstances discussed above.

RESULTS

Section 1: Bone Analyses

Procrustes ANOVA revealed significant interactions between shape and sex (cranium $p = 0.002$, mandible $p = 0.067$), so male and female results are presented independently.

Female Data

In the cranium, we found that significant shape differences ($p = 0.001$) existed between edentate and dentate females (Table 6). The first two principal components contributed 44.19% of the total shape variation between groups (Figure 3). PC1 represented alveolar resorption and contributed 26.81% of the total shape variance between groups. The changes around the orbit and at nasion can be explained by a total decrease in facial height due to alveolar resorption. PC2 (17.38%) represented palatal narrowing and shortening.

In the mandible, we found that significant shape differences ($p = 0.001$) existed between edentate and dentate females (Table 6). The first three principal components contributed 68.43% of the total shape variation between groups (Figure 4). PC1 (43.99%) represented alveolar resorption. PC2 (15.09%) represented a drift of the mandibular corpus towards midline, particularly in the superior border, thus leading to a narrowing of the mandible as a whole. PC3 (9.35%) represented a superior elongation and posterior retraction of the coronoid process, the site at which the temporalis muscle attaches to the mandible.

Figure 3: PCA of Female Crania – Bar graph (top) represents the proportion of variance contributed by each principal component to the total shape variance between groups. Scatter plot (middle left) represents the distribution of individuals for each principal component. Lollipop graphs (middle right, bottom) represent the direction of shape differences between groups, with the sphere as the mean shape and the stick as the direction in which edentulous individuals differ from that mean.

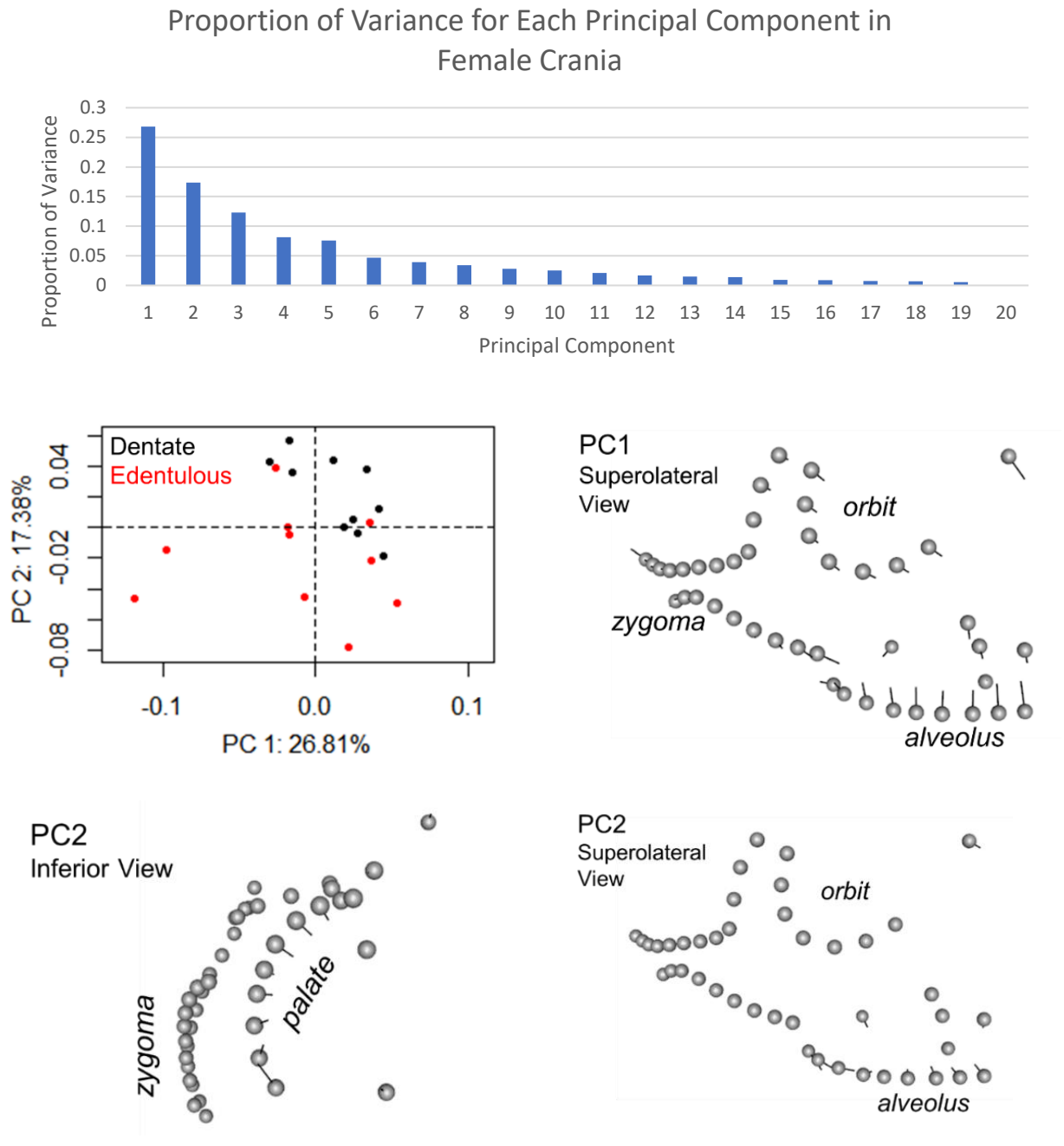

Figure 4: PCA of Female Mandibles – Bar graph (top) represents the proportion of variance contributed by each principal component to the total shape variance between groups. Scatter

plots (middle) represent the distribution of individuals for each principal component. Lollipop graphs (bottom) represent the direction of shape differences between groups, with the sphere as the mean shape and the stick as the direction in which edentulous individuals differ from that mean.

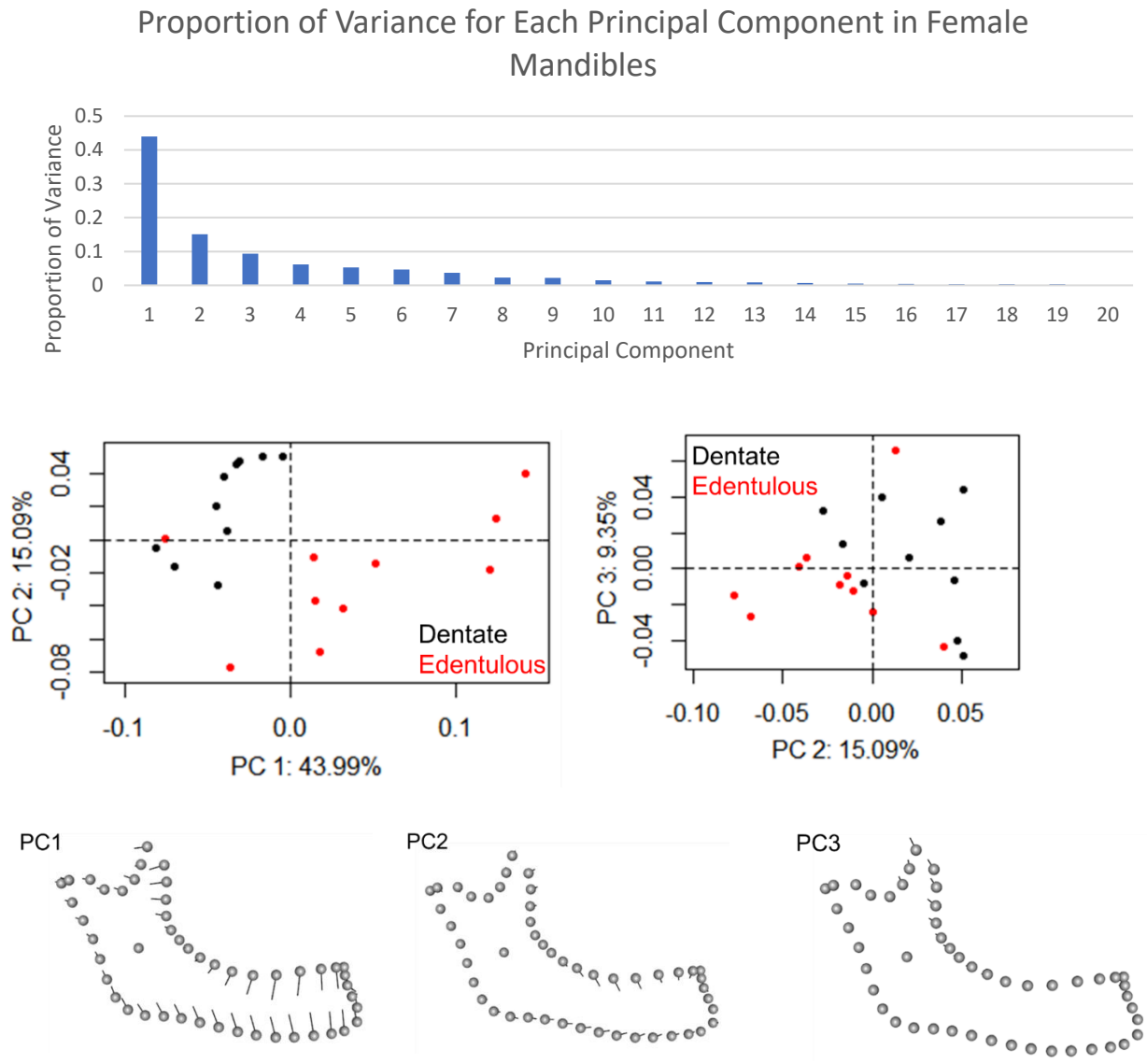

Male Data

In the cranium, we found that significant shape differences (p = 0.001) existed between edentate and dentate males (Table 6). The first three principal components contributed 56.48% of the total shape variation between groups (Figure 5). PC1 (26.81%) represented palatal narrowing and shortening. PC2 (17.38%) represented a narrowing of the anterior zygomatic root, the site at which the superficial masseter attaches to the cranium. PC3 (12.29%) represented vertical alveolar resorption, particularly at the molars.

In the mandible, we found that significant shape differences (p = 0.002) existed between edentate and dentate males (Table 6). The first three principal components contributed 72.29% of the total shape variation between groups (Figure 6). PC1 (42.80%) represented alveolar resorption. PC2 (17.24%) represented a drift of the mandibular corpus towards midline, particularly in the superior border, thus leading to a narrowing of the mandible as a whole. PC3 (12.25%) represented a superior elongation and posterior retraction of the coronoid process, the site at which the temporalis muscle attaches to the mandible.

Figure 5: PCA of Male Crania– Bar graph (top) represents the proportion of variance contributed by each principal component to the total shape variance between groups. Scatter plots (row 2) represent the distribution of individuals for each principal component. Lollipop graphs (rows 3-4) represent the direction of shape differences between groups, with the sphere as the mean shape and the stick as the direction in which edentulous individuals differ from that mean.

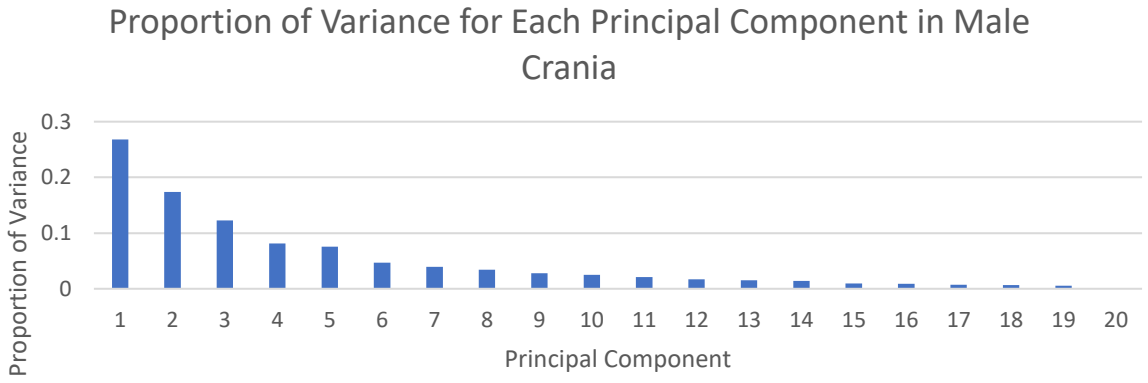

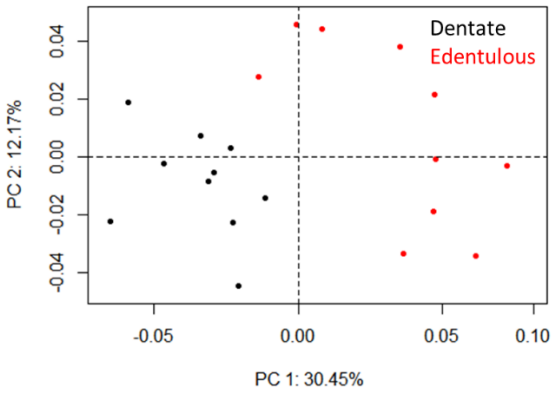
Dentate
Edentulous
PC 2: 12.17%
PC 1: 30.45%
0.04
0.02
0.00
-0.02
-0.04
-0.05
0.00
0.05
0.10

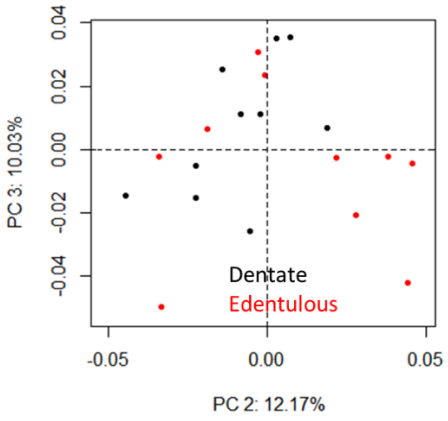
Dentate
Edentulous
PC 3: 10.03%
PC 2: 12.17%
0.04
0.02
0.00
-0.02
-0.04
-0.05
0.00
0.05

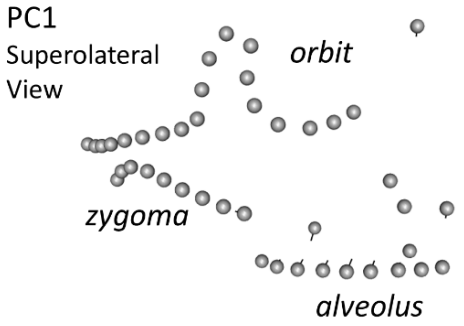
PC1
Superolateral
View
orbit
zygoma
alveolus

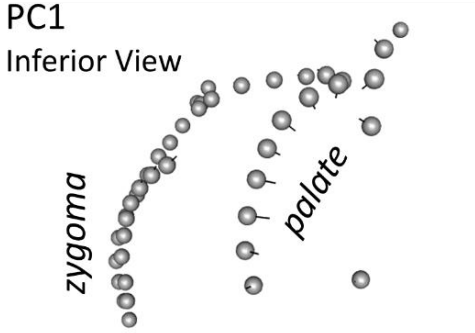
PC1
Inferior View
zygoma
palate

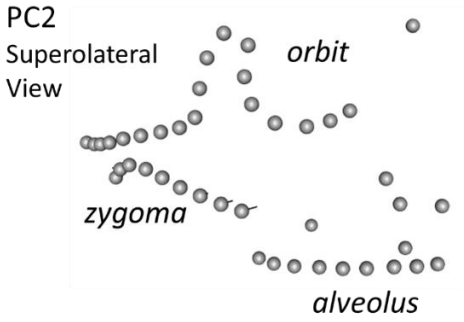
PC2
Superolateral
View
orbit
zygoma
alveolus

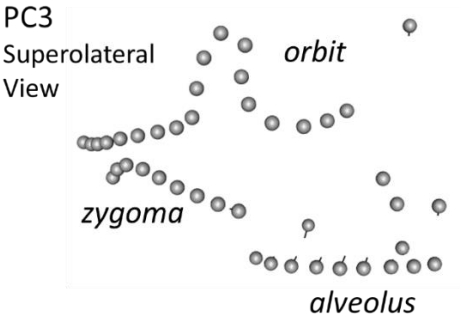
PC3
Superolateral
View
orbit
zygoma
alveolus

Figure 6: PCA of Male Mandible – Bar graph (top) represents the proportion of variance contributed by each principal component to the total shape variance between groups. Scatter plots (middle) represent the distribution of individuals for each principal component. Lollipop graphs (bottom) represent the direction of shape differences between groups, with the sphere as the mean shape and the stick as the direction in which edentulous individuals differ from that mean.

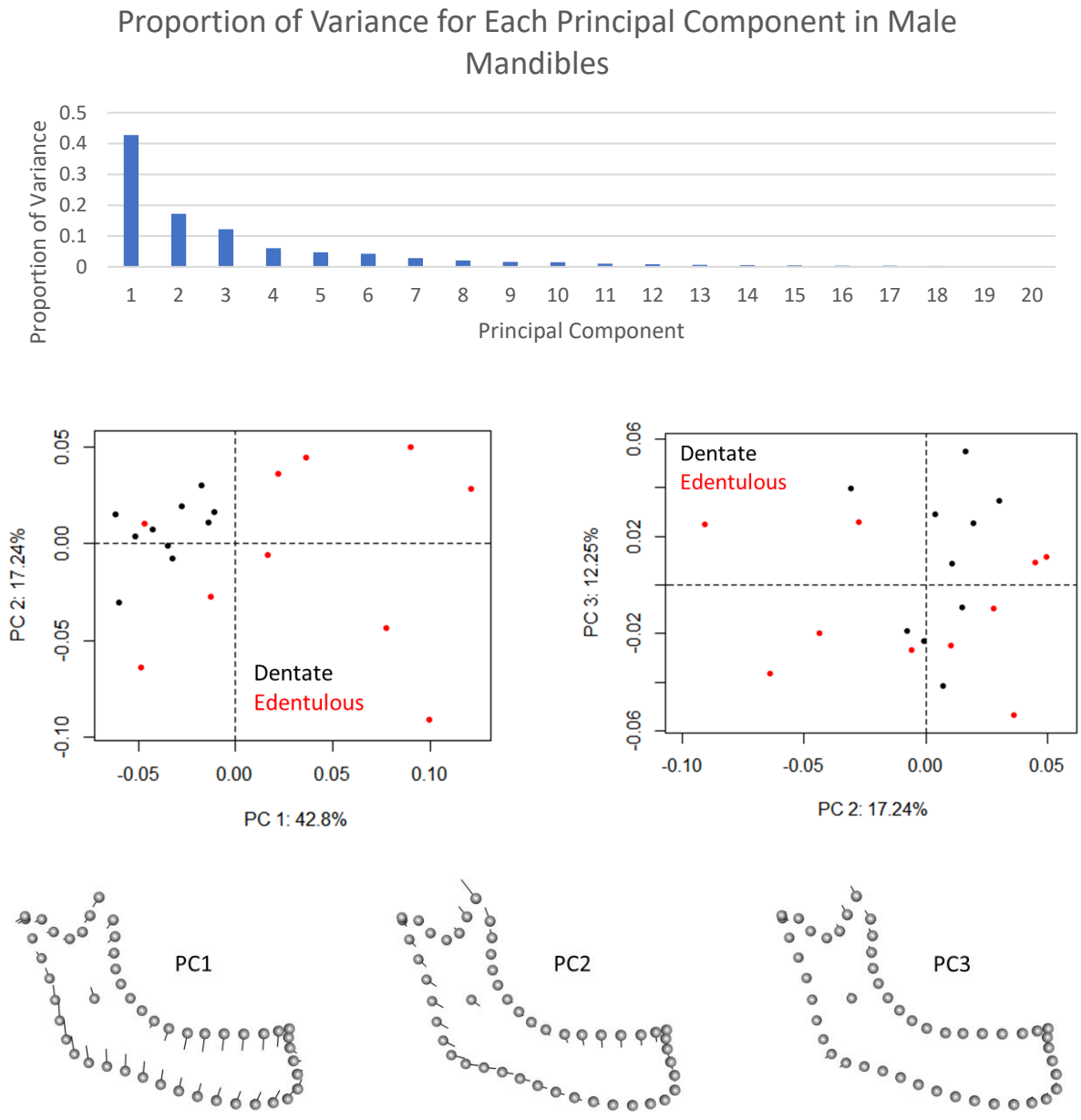

Table 6: ANOVA for Shape Differences between Dentate and Edentate

	R Squared	**P value**
Female Cranium	0.1373	0.001
Female Mandible	0.23382	0.001
Male Cranium	0.2423	0.001
Male Mandible	0.2009	0.002

Section 2: Muscle Analyses

While fiber type analysis was not possible, several qualitative observations were made of the masseter tissue. Edentate masseters were much thinner than dentate masseters, suggesting that edentate masseters have undergone greater muscle atrophy. Additionally, H&E-stained masseter tissue revealed fat infiltration between muscle fibers, particularly in edentate specimens (Figure 7).

Figure 7: Masseter H&E Staining

Dentate, 10x

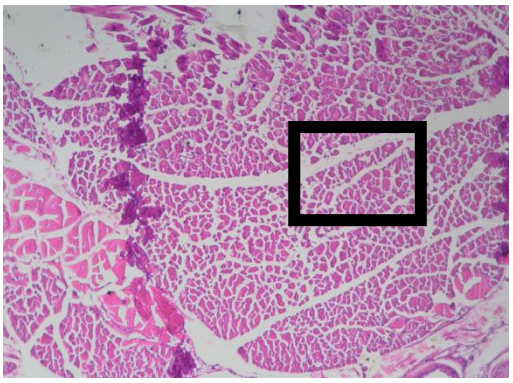

Dentate, 40x

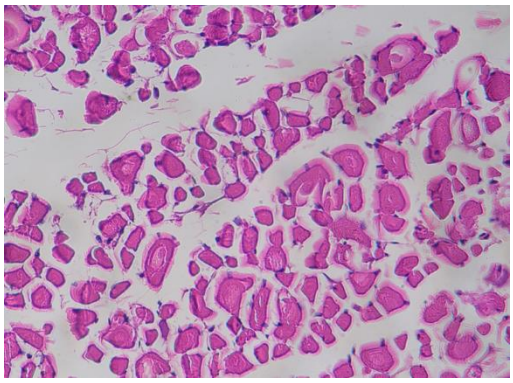

Edentate without fat infiltration, 10x

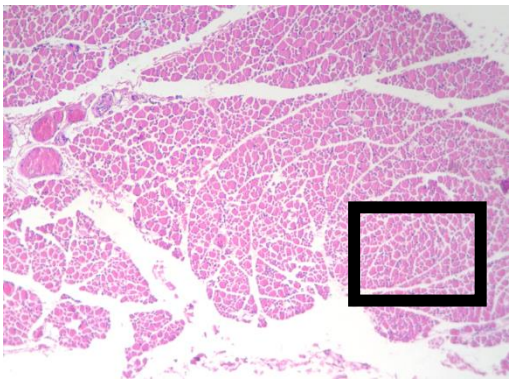

Edentate without fat infiltration, 40x

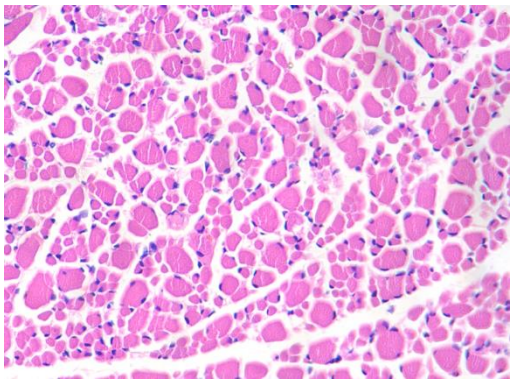

Edentate with fat infiltration, 10x

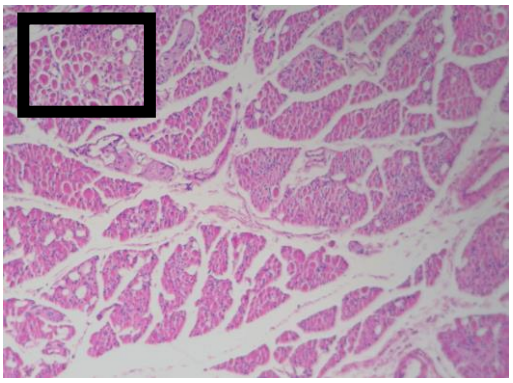

Edentate with fat infiltration, 40x

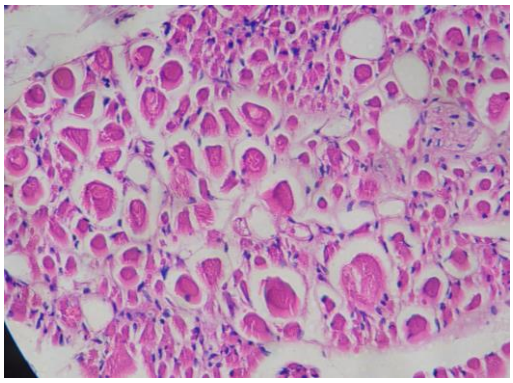

DISCUSSION

The data show that cranial and mandibular shapes were significantly different between edentate and dentate individuals. While shape changes follow similar patterns between sexes, the magnitude of these changes differ between males and females.

Alveolar Shape Changes

Vertical alveolar resorption accounts for the largest shape difference between edentate and dentate females, but palatal narrowing accounts for the largest shape difference between edentate and dentate males. In females, alveolar resorption in the maxilla resulted in a shorter face. Changes around the orbit and nasion were in the same principal component as alveolar resorption, indicating that these shape changes are linked.[1] In males, vertical alveolar resorption was not as pronounced in edentate individuals, but most significant in the posterior palate at the molars. Furthermore, alveolar resorption in the maxilla resulted in a narrower and shorter palate in both males and females. Alveolar resorption in the mandible resulted in a vertically shorter mandibular corpus and narrower mandible in both males and females. These findings are consistent with previous studies that showed that the rate of resorption is greater at the buccal surface as compared to the lingual surface, but also noted that the degree of buccal resorption was noted to be greater at the molars than at the premolars or incisors, which would produce a narrowing of both the palate and mandible.[8]

Two edentate females were outliers, showing much more alveolar resorption along the maxilla than other edentate females, thus possibly driving PC1 in the female crania. In fact, removing these two outlier female edentate crania resulted in a trend that looked more similar to

that of male crania, with PC1 representing palatal narrowing and shortening and PC2 representing vertical alveolar resorption. The deviations between male and female craniofacial shape changes may also be explained by the fact female craniofacial dimensions are smaller on average, so any significant amount of tooth loss may lead to a seemingly larger change in facial shape. Among edentate males, there was clear evidence of denture usage in the CT images. While the effects of denture wearing on alveolar resorption were not examined in this study, it is possible that this behavior could lead to decreased alveolar resorption and thus smaller change in craniofacial dimensions.

Figure 8: Examples of Phenotypic Variance Among Edentate Individuals

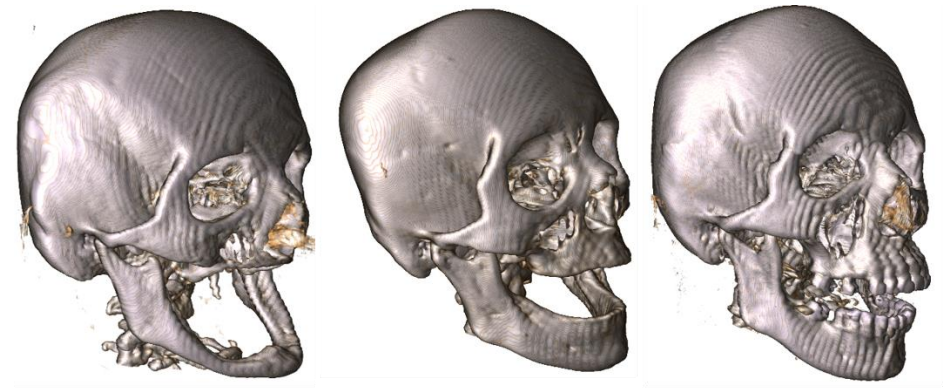

In fact, among edentate individuals, there was a wide range of craniofacial phenotypes (Figure 8). In some edentate individuals, there is clear, visually observable evidence of alveolar resorption, while in other edentate individuals, there are few if any signs of alveolar resorption. The range of morphology observed in edentate individuals is most likely due to time since tooth loss – alveolar resorption is a time-dependent process, so an individual who became edentate shortly before death would show little evidence of alveolar resorption in post-mortem CT

imaging. This range could also potentially be explained by certain behaviors, particularly denture usage – those who use dentures more regularly may experience a smaller degree of alveolar resorption. There may also be a sex component to denture-wearing behavior. Elderly females report lower rates of satisfaction with the aesthetics and chew performance of their dentures.[37] Elderly females also reported higher rates of ulceration and oral inflammation as a result of wearing dentures, thus suggesting that overall compliance in denture wearing may be lower among females.[38] While this study did not attempt to quantify the impact of behavioral factors such as denture wearing or other factors including socioeconomic status and smoking, these are all potentially interesting targets of future investigation.

Muscle Attachment Site Shape Changes

No change was seen at the free portion of the zygomatic arch, the attachment site of the deep masseter, suggesting that its role in maintaining the mandibular position against gravity is unchanged. This is consistent with previous findings regarding the zygomatic arch.[1] However, the narrowing of the anterior zygomatic root in edentate males demonstrates that a differential atrophy of the superficial masseter may occur relative to the deep masseter. One possible cause of this could be a reduction in jaw protraction movements, such as those used in transverse grinding or mastication, in edentate individuals.[39]

Qualitative observation of H&E stained of masseter specimens showed that the muscle fibers of edentate individuals were atrophied relative to dentate individuals. Furthermore, several edentate specimens had adipocytes interposed between muscle fibers, showing that some level of fat infiltration was occurring.

The coronoid process, the attachment site of the temporalis muscle, was posteriorly displaced and vertically elongated. The significance is unclear and warrants further study. Future directions of study include landmarking along the attachment lines of the temporalis as well as muscle fiber histology of the temporalis.

Future studies will investigate the changes seen in the structure and physiology of the masticatory muscles following tooth loss. We hope that our work will shed light on the functional differences between the masseter and temporalis muscles following tooth loss, and ultimately help us better understand musculoskeletal atrophy and bone loss during aging- and disease-related tooth loss.

CONCLUSIONS

Significant differences in facial and mandibular shape exist between dentate and edentate individuals. These shape differences follow similar trends in males and females, but the magnitude of these differences varies between the sexes. Variation within edentulous individuals suggests that the time since tooth loss and behavioral factors (e.g. denture wearing) may impact the degree of alveolar resorption. Further investigation is needed to evaluate the effect of dentures and implants on craniofacial shape changes.

A superior elongation and posterior retraction of the coronoid process was observed in edentulous individuals, suggesting greater relative atrophy of the temporalis muscle relative to the masseter following tooth loss. Future studies are needed to understand how the masseter and the temporalis muscles change following tooth loss.

BIBLIOGRAPHY

1 Small, C., Brits, D. & Hemingway, J. Assessing the effects of tooth loss in adult crania using geometric morphometrics. *Int J Legal Med* **130**, 233-243, doi:10.1007/s00414-015-1174-6 (2016).

2 Bodic, F., Hamel, L., Lerouxel, E., Basle, M. F. & Chappard, D. Bone loss and teeth. *Joint Bone Spine* **72**, 215-221, doi:10.1016/j.jbspin.2004.03.007 (2005).

3 Williams, S. E. & Slice, D. E. Regional shape change in adult facial bone curvature with age. *Am J Phys Anthropol* **143**, 437-447, doi:10.1002/ajpa.21332 (2010).

4 Kloss, F. R. & Gassner, R. Bone and aging: effects on the maxillofacial skeleton. *Exp Gerontol* **41**, 123-129, doi:10.1016/j.exger.2005.11.005 (2006).

5 Crothers, A. J. Tooth wear and facial morphology. *J Dent* **20**, 333-341, doi:10.1016/0300-5712(92)90019-9 (1992).

6 Heath, M. R. A cephalometric study of the middle third of the adult human face related to age and the loss of dental tissue. *Arch Oral Biol* **11**, 677-686, doi:10.1016/0003-9969(66)90093-8 (1966).

7 Dechow, P. C., Wang, Q. & Peterson, J. Edentulation alters material properties of cortical bone in the human craniofacial skeleton: functional implications for craniofacial structure in primate evolution. *Anat Rec (Hoboken)* **293**, 618-629, doi:10.1002/ar.21124 (2010).

8 Pietrokovski, J. & Massler, M. Alveolar ridge resorption following tooth extraction. *J Prosthet Dent* **17**, 21-27, doi:10.1016/0022-3913(67)90046-7 (1967).

9 Lestrel, P. E., Kapur, K. K. & Chauncey, H. H. A cephalometric study of mandibular cortical bone thickness in dentulous persons and denture wearers. *J Prosthet Dent* **43**, 89-94, doi:10.1016/0022-3913(80)90360-1 (1980).

10 Staron, R. S. Human skeletal muscle fiber types: delineation, development, and distribution. *Can J Appl Physiol* **22**, 307-327, doi:10.1139/h97-020 (1997).

11 Scott, W., Stevens, J. & Binder-Macleod, S. A. Human skeletal muscle fiber type classifications. *Phys Ther* **81**, 1810-1816 (2001).

12 McComas, A. J. *Skeletal muscle : form and function*. (Human Kinetics, 1996).

13 Pette, D., Peuker, H. & Staron, R. S. The impact of biochemical methods for single muscle fibre analysis. *Acta Physiol Scand* **166**, 261-277, doi:10.1046/j.1365-201x.1999.00568.x (1999).

14 Esbjornsson, M. E., Dahlstrom, M. S., Gierup, J. W. & Jansson, E. C. Muscle fiber size in healthy children and adults in relation to sex and fiber types. *Muscle Nerve* **63**, 586-592, doi:10.1002/mus.27151 (2021).

15 Pette, D. & Staron, R. S. Mammalian skeletal muscle fiber type transitions. *Int Rev Cytol* **170**, 143-223, doi:10.1016/s0074-7696(08)61622-8 (1997).

16 Burke, R. E. Revisiting the notion of 'motor unit types'. *Prog Brain Res* **123**, 167-175 (1999).

17 Ricoy, J. R., Encinas, A. R., Cabello, A., Madero, S. & Arenas, J. Histochemical study of the vastus lateralis muscle fibre types of athletes. *J Physiol Biochem* **54**, 41-47 (1998).

18

Kraemer, W. J., Fleck, S. J. & Evans, W. J. Strength and power training: physiological mechanisms of adaptation. *Exerc Sport Sci Rev* **24**, 363-397 (1996).
19 Holloszy, J. O. & Booth, F. W. Biochemical adaptations to endurance exercise in muscle. *Annu Rev Physiol* **38**, 273-291, doi:10.1146/annurev.ph.38.030176.001421 (1976).
20 Porter, M. M., Vandervoort, A. A. & Lexell, J. Aging of human muscle: structure, function and adaptability. *Scand J Med Sci Sports* **5**, 129-142, doi:10.1111/j.1600-0838.1995.tb00026.x (1995).
21 Roos, M. R., Rice, C. L. & Vandervoort, A. A. Age-related changes in motor unit function. *Muscle Nerve* **20**, 679-690, doi:10.1002/(sici)1097-4598(199706)20:6<679::aid-mus4>3.0.co;2-5 (1997).
22 Lexell, J., Taylor, C. C. & Sjostrom, M. What is the cause of the ageing atrophy? Total number, size and proportion of different fiber types studied in whole vastus lateralis muscle from 15- to 83-year-old men. *J Neurol Sci* **84**, 275-294, doi:10.1016/0022-510x(88)90132-3 (1988).
23 Kamen, G., Sison, S. V., Du, C. C. & Patten, C. Motor unit discharge behavior in older adults during maximal-effort contractions. *J Appl Physiol (1985)* **79**, 1908-1913, doi:10.1152/jappl.1995.79.6.1908 (1995).
24 Andersen, J. L., Terzis, G. & Kryger, A. Increase in the degree of coexpression of myosin heavy chain isoforms in skeletal muscle fibers of the very old. *Muscle Nerve* **22**, 449-454, doi:10.1002/(sici)1097-4598(199904)22:4<449::aid-mus4>3.0.co;2-2 (1999).
25 Miljkovic, N., Lim, J. Y., Miljkovic, I. & Frontera, W. R. Aging of skeletal muscle fibers. *Ann Rehabil Med* **39**, 155-162, doi:10.5535/arm.2015.39.2.155 (2015).
26 Korfage, J. A., Koolstra, J. H., Langenbach, G. E. & van Eijden, T. M. Fiber-type composition of the human jaw muscles--(part 1) origin and functional significance of fiber-type diversity. *J Dent Res* **84**, 774-783, doi:10.1177/154405910508400901 (2005).
27 Monemi, M., Eriksson, P. O., Kadi, F., Butler-Browne, G. S. & Thornell, L. E. Opposite changes in myosin heavy chain composition of human masseter and biceps brachii muscles during aging. *J Muscle Res Cell Motil* **20**, 351-361, doi:10.1023/a:1005421604314 (1999).
28 Korfage, J. A., Koolstra, J. H., Langenbach, G. E. & van Eijden, T. M. Fiber-type composition of the human jaw muscles--(part 2) role of hybrid fibers and factors responsible for inter-individual variation. *J Dent Res* **84**, 784-793, doi:10.1177/154405910508400902 (2005).
29 Korfage, J. A., Schueler, Y. T., Brugman, P. & Van Eijden, T. M. Differences in myosin heavy-chain composition between human jaw-closing muscles and supra- and infrahyoid muscles. *Arch Oral Biol* **46**, 821-827, doi:10.1016/s0003-9969(01)00042-5 (2001).
30 Kitagawa, Y. *et al.* Maxillofacial Deformity and Change in the Histochemical Characteristics of the Masseter Muscle after Unilateral Sectioning of the Facial Nerve in Growing Rabbits. *Acta Histochemica Et Cytochemica - ACTA HISTOCHEM CYTOCHEM* **35**, 305-313, doi:10.1267/ahc.35.305 (2002).
31 Kiliaridis, S., Engstrom, C. & Thilander, B. Histochemical analysis of masticatory muscle in the growing rat after prolonged alteration in the consistency of the diet. *Arch Oral Biol* **33**, 187-193, doi:10.1016/0003-9969(88)90044-1 (1988).
32 Maxwell, L. C., McNamara, J. A., Jr., Carlson, D. S. & Faulkner, J. A. Histochemistry of fibres of masseter and temporalis muscles of edentulous monkeys Macaca mulatta. *Arch Oral Biol* **25**, 87-93, doi:10.1016/0003-9969(80)90082-5 (1980).
33 Langenbach, G., van de Pavert, S., Savalle, W., Korfage, H. & van Eijden, T. Influence of food consistency on the rabbit masseter muscle fibres. *Eur J Oral Sci* **111**, 81-84, doi:10.1034/j.1600-0722.2003.00008.x (2003).
34 Ravosa, M. J. *et al.* Masticatory biomechanics and masseter fiber-type plasticity. *J Musculoskelet Neuronal Interact* **10**, 46-55 (2010).
35 LaRocque, H., Rossiter, J. A. & Menegaz, R. A. Dietary Effects on Fiber Type Plasticity in the Masseter Muscle. *The FASEB Journal* **34**, 1-1, doi:10.1096/fasebj.2020.34.s1.03002 (2020).

36 Kasai, K., Richards, L. C., Kanazawa, E., Ozaki, T. & Iwasawa, T. Relationship between attachment of the superficial masseter muscle and craniofacial morphology in dentate and edentulous humans. *J Dent Res* **73**, 1142-1149, doi:10.1177/00220345940730060301 (1994).
37 Pan, S. *et al.* Sex differences in denture satisfaction. *J Dent* **36**, 301-308, doi:10.1016/j.jdent.2008.02.009 (2008).
38 Baran, I. & Nalcaci, R. Self-reported denture hygiene habits and oral tissue conditions of complete denture wearers. *Arch Gerontol Geriatr* **49**, 237-241, doi:10.1016/j.archger.2008.08.010 (2009).
39 Hylander, W. Functional anatomy and biomechanics of the masticatory apparatus. *Temporomandibular Disorders: an Evidenced Approach to Diagnosis and Treatment*, 1-34 (2006).

APPENDIX A

Table A: Complete PCA Tables

Female Cranium			
Principal Component	**Eigenvalues**	**Proportion of Variance**	**Cumulative Proportion**
Comp1	0.002058398	0.268055697	0.268055697
Comp2	0.001334645	0.173804701	0.441860398
Comp3	0.000943724	0.122896868	0.564757266
Comp4	0.000624432	0.081316891	0.646074158
Comp5	0.000581812	0.075766707	0.721840865
Comp6	0.000358761	0.046719823	0.768560688
Comp7	0.000302137	0.039345946	0.807906634
Comp8	0.000261461	0.034048826	0.84195546
Comp9	0.00021485	0.027978908	0.869934368
Comp10	0.000193225	0.025162855	0.895097223
Comp11	0.000160064	0.020844358	0.915941581
Comp12	0.000129713	0.016891885	0.932833466
Comp13	0.000116056	0.015113434	0.9479469
Comp14	0.00010767	0.014021359	0.961968259
Comp15	7.15E-05	9.31E-03	9.71E-01

Comp16	6.90E-05	8.99E-03	9.80E-01
Comp17	5.67E-05	7.38E-03	9.88E-01
Comp18	5.20E-05	6.77E-03	9.94E-01
Comp19	4.29E-05	5.58E-03	1.00E+00
Comp20	1.97E-33	2.56E-31	1.00E+00
Female Mandible			
Principal Component	**Eigenvalues**	**Proportion of Variance**	**Cumulative Proportion**
Comp1	0.004368626	0.439873948	0.439873948
Comp2	0.001498558	0.150888787	0.590762734
Comp3	0.000928466	0.093486554	0.684249289
Comp4	0.000616693	0.062094394	0.746343683
Comp5	0.000529242	0.053288998	0.79963268
Comp6	0.000466404	0.046961891	0.846594571
Comp7	0.000370712	0.037326765	0.883921336
Comp8	0.000229892	0.023147701	0.907069037
Comp9	0.000217284	0.021878125	0.928947162
Comp10	0.000149123	0.015015123	0.943962285
Comp11	0.000111509	0.011227807	0.955190092
Comp12	9.78628E-05	0.009853738	0.96504383
Comp13	9.08E-05	9.14E-03	9.74E-01
Comp14	7.08E-05	7.13E-03	9.81E-01

Comp15	4.80E-05	4.83E-03	9.86E-01
Comp16	4.30E-05	4.33E-03	9.90E-01
Comp17	3.31E-05	3.34E-03	9.94E-01
Comp18	3.09E-05	3.11E-03	9.97E-01
Comp19	3.05E-05	3.07E-03	1.00E+00
Comp20	2.31E-33	2.33E-31	1.00E+00
Male Cranium			
Principal Component	**Eigenvalues**	**Proportion of Variance**	**Cumulative Proportion**
Comp1	0.002058398	0.268055697	0.268055697
Comp2	0.001334645	0.173804701	0.441860398
Comp3	0.000943724	0.122896868	0.564757266
Comp4	0.000624432	0.081316891	0.646074158
Comp5	0.000581812	0.075766707	0.721840865
Comp6	0.000358761	0.046719823	0.768560688
Comp7	0.000302137	0.039345946	0.807906634
Comp8	0.000261461	0.034048826	0.84195546
Comp9	0.00021485	0.027978908	0.869934368
Comp10	0.000193225	0.025162855	0.895097223
Comp11	0.000160064	0.020844358	0.915941581
Comp12	0.000129713	0.016891885	0.932833466
Comp13	0.000116056	0.015113434	0.9479469

Comp14	0.00010767	0.014021359	0.961968259
Comp15	7.15E-05	9.31E-03	9.71E-01
Comp16	6.90E-05	8.99E-03	9.80E-01
Comp17	5.67E-05	7.38E-03	9.88E-01
Comp18	5.20E-05	6.77E-03	9.94E-01
Comp19	4.29E-05	5.58E-03	1.00E+00
Comp20	1.97E-33	2.56E-31	1.00E+00
Male Mandible			
Principal Component	**Eigenvalues**	**Proportion of Variance**	**Cumulative Proportion**
Comp1	0.003218987	0.427963535	0.427963535
Comp2	0.00129709	0.17244773	0.60041127
Comp3	0.000921252	0.122480235	0.722891502
Comp4	0.000452101	0.060106755	0.782998257
Comp5	0.000357357	0.047510456	0.830508712
Comp6	0.000316892	0.04213074	0.872639452
Comp7	0.000215891	0.028702631	0.901342083
Comp8	0.000155397	0.020659983	0.922002066
Comp9	0.00011753	0.015625616	0.937627682
Comp10	0.000114503	0.015223156	0.952850839
Comp11	7.48E-05	9.95E-03	9.63E-01
Comp12	6.35E-05	8.45E-03	9.71E-01

Comp13	4.99E-05	6.63E-03	9.78E-01
Comp14	4.45E-05	5.91E-03	9.84E-01
Comp15	3.51E-05	4.67E-03	9.88E-01
Comp16	2.83E-05	3.76E-03	9.92E-01
Comp17	2.65E-05	3.53E-03	9.96E-01
Comp18	1.84E-05	2.45E-03	9.98E-01
Comp19	1.36E-05	1.80E-03	1.00E+00
Comp20	2.04E-33	2.72E-31	1.00E+00

APPENDIX B

Figure B: Full-Size Figures of Craniofacial Landmarks

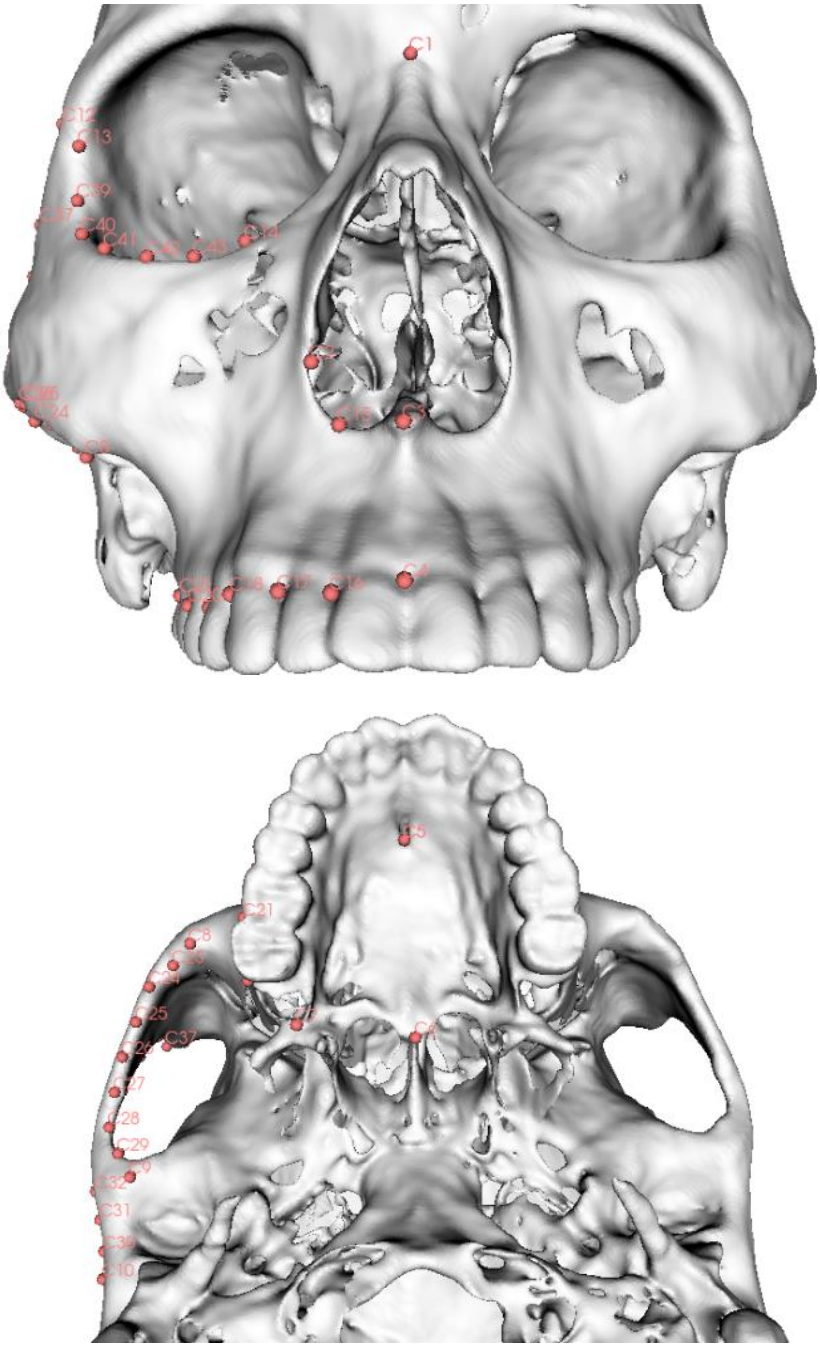

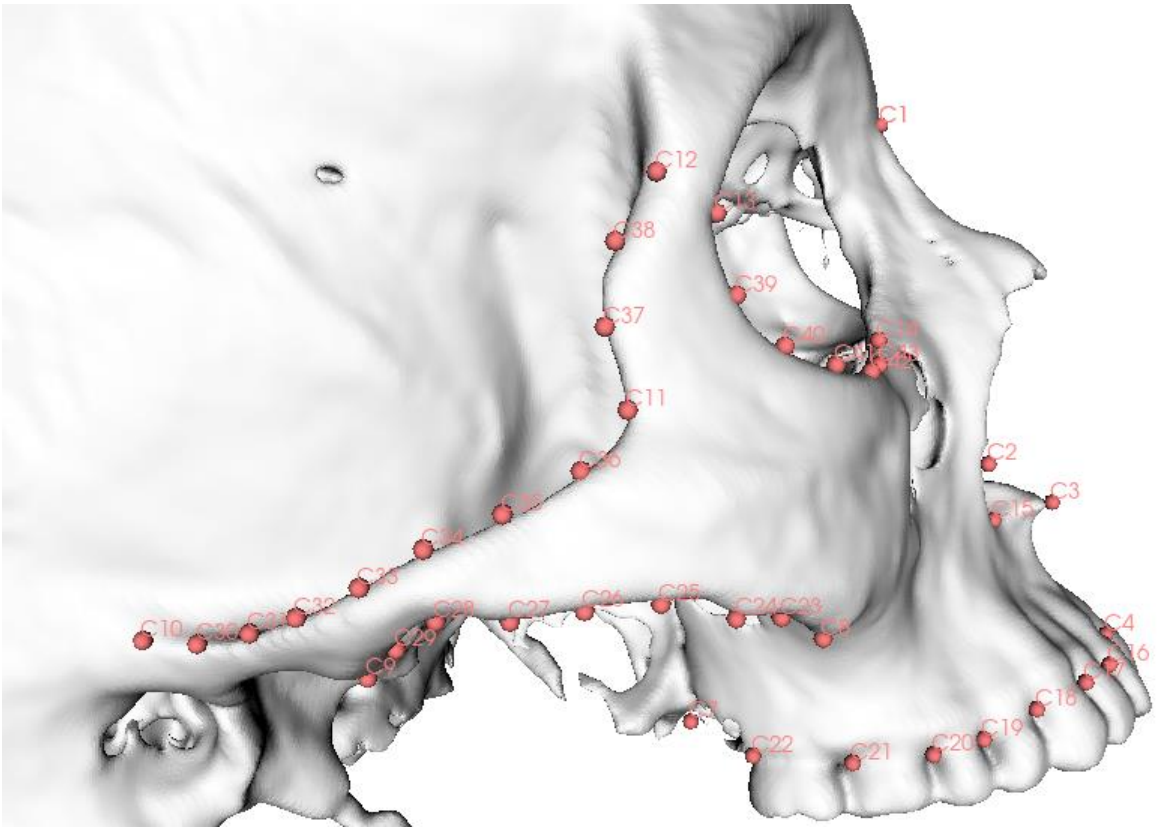
C1
C12
C38
C39
C37
C11
C2
C3
C4
C16
C19
C20
C21
C22
C10
C9
C29
C27
C24
C23

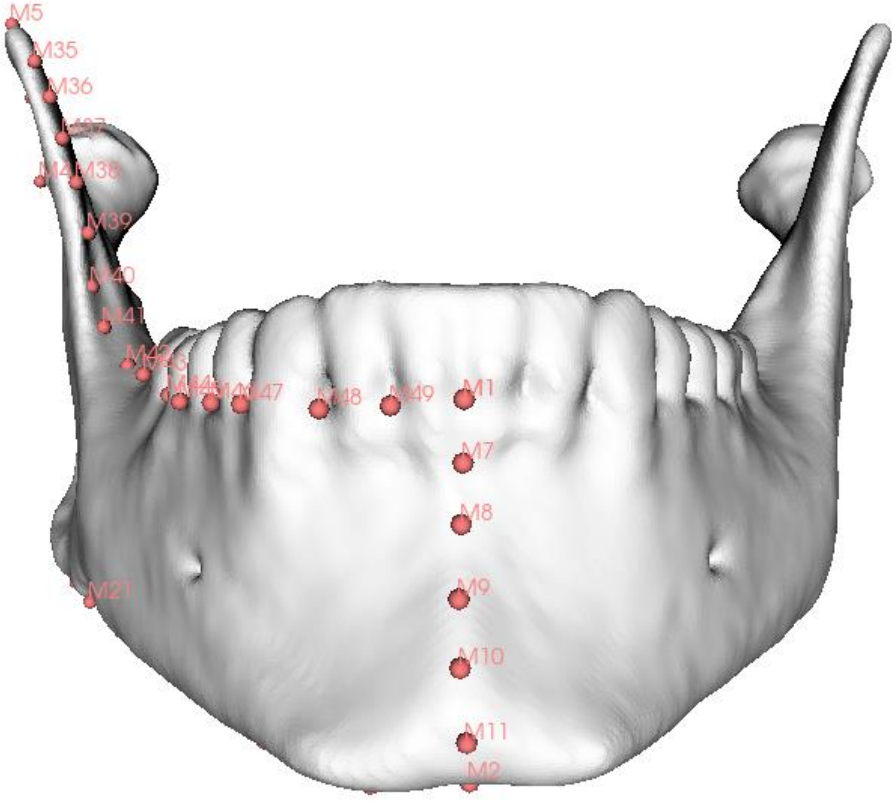
M5
M35
M36
M38
M39
M40
M41
M47
M48
M49
M1
M7
M8
M21
M9
M10
M11
M2

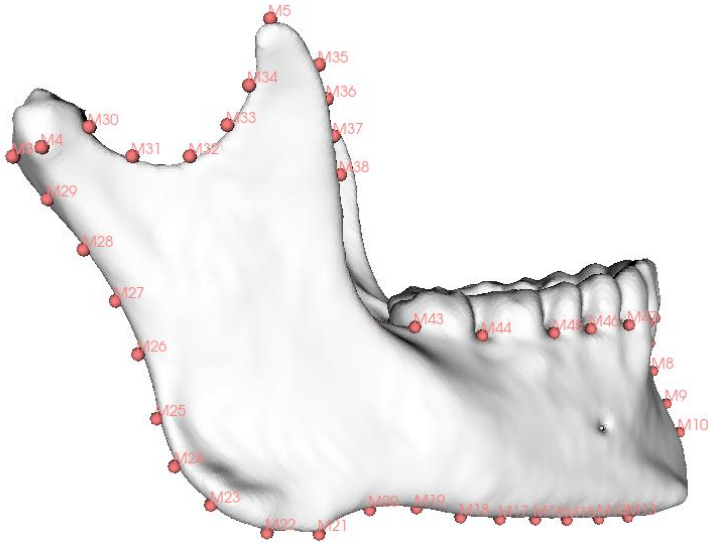
M5
M35
M34
M36
M30
M33
M37
M4
M31
M32
M38
M29
M28
M27
M43
M44
M26
M18
M9
M25
M10
M24
M23
M22
M21

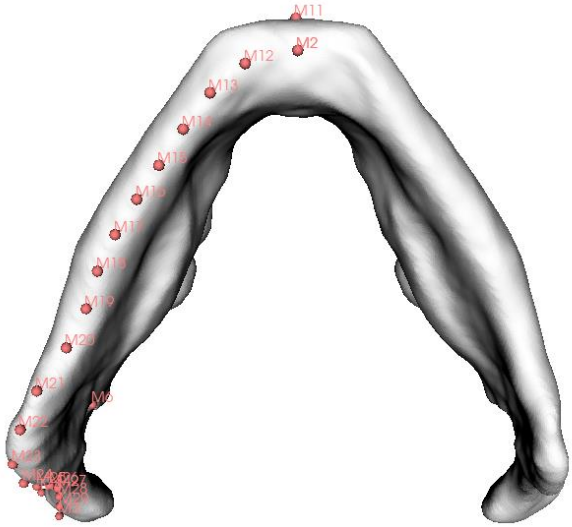
M11
M2
M12
M13
M14
M15
M16
M17
M18
M19
M20
M21

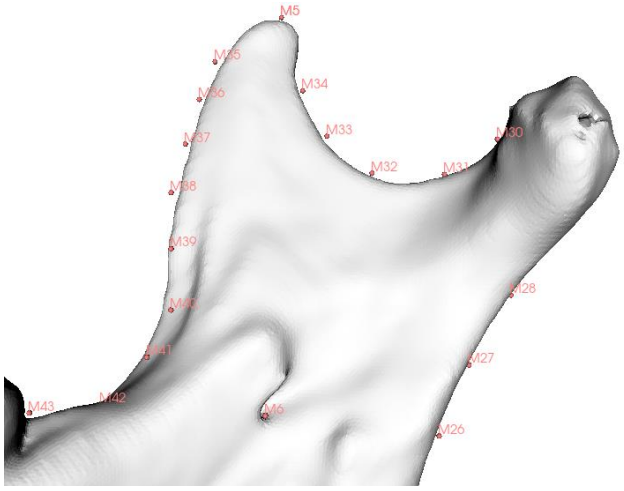
M5
M35
M34
M36
M33
M37
M30
M32
M31
M38
M39
M28
M40
M27
M41
M43
M42
M6
M26